

Miscibility and Intermolecular Hydrogen-bonding Interactions in Poly(3-hydroxybutyrate-co-3-hydroxyhexanoate)/Poly(4-vinyl phenol) Binary Blends

Hexig Alata, Bo Zhu, Yoshio Inoue

Department of Biomolecular Engineering, Tokyo Institute of Technology, Midori-ku, Yokohama 226-8501, Japan

Received 21 February 2007; accepted 23 May 2007

DOI 10.1002/app.26884

Published online 20 July 2007 in Wiley InterScience (www.interscience.wiley.com).

ABSTRACT: The miscibility and hydrogen bonding interaction in the poly(3-hydroxybutyrate-co-3-hydroxyhexanoate)/poly(4-vinyl phenol) [P(3HB-co-3HH)/PVPh] binary blends were investigated by differential scanning calorimetry (DSC) and Fourier transform infrared spectroscopy (FTIR). The DSC results indicate that P(3HB-co-3HH) with 20 mol % 3HH unit content is fully miscible with PVPh, and FTIR studies reveal the existence of hydrogen

bonding interaction between the carbonyl groups of P(3HB-co-3HH) and the hydroxyl groups of PVPh. The effect of blending of PVPh on the mechanical properties of P(3HB-co-3HH) were studied by tensile testing. © 2007 Wiley Periodicals, Inc. *J Appl Polym Sci* 106: 2025–2030, 2007

Key words: polymer blends; hydrogen bonds; P(3HB-co-3HH); PVPh

INTRODUCTION

Blending offers a more attractive and alternative method to create new polymeric materials than developing totally new polymers.^{1–3} In the last two decades, with the increasing concern about the environmental and energy problems, a great attention has been paid on environmentally friendly thermoplastic materials and their blend systems in polymer science.^{4,5} A series of natural polyesters polyhydroxyalkanoates (PHAs) including poly(3-hydroxybutyrate) (PHB) and its copolymers, produced by a wide variety of microorganisms as intracellular reserve materials, are receiving an increasing attention for possible application as biodegradable, melt processable polymers, which can be produced from renewable resources. To improve mechanical properties and reduce the production cost, incorporation of other monomer units into the P(3HB) chain to form copolymers and blending with synthetic polymers have been widely performed. A series of random copolymers containing 3-hydroxybutyrate (3HB) unit have been produced by microorganisms, such as poly(3-hydroxybutyrate-co-3-hydroxyvalerate) [P(3HB-co-3HV)],⁶ poly(3-hydroxybutyrate-co-3-hydroxyhexanoate) [P(3HB-co-3HH)],⁷ poly(3-hydroxybutyrate-co-3-hydroxypropionate) [P(3HB-co-3HP)],⁸ and poly(3-hydroxybutyrate-co-4-hydroxybutyrate) [P(3HB-co-4HB)].⁹

P(3HB) formed miscible blends with various commercial polymers such as poly(ethylene oxide),^{10,11} poly(vinylidene fluoride),^{12,13} poly(vinyl chloride),^{14,15} poly(epichlorohydrin),^{16,17} poly(4-vinylphenol) (PVPh),¹⁸ and poly(vinyl acetate).^{19,20} P(3HB-co-3HH), as a new member of the PHA family, is produced on a large scale.^{7,21} P(3HB-co-3HH) has significantly different properties when compared with PHB because of the long chain branching, and is a good candidate for the clinical biomaterials. However, the low glass transition temperature limited the manufacturability of P(3HB-co-3HH).²²

In previous works, much attention has been paid to the miscibility of PVPh with other polymers.^{23–27} PVPh can act as a proton donor that forms a strong intermolecular hydrogen bond with proton acceptor such as carbonyl, ether, or other functional groups of the second polymers. A variety of binary blends containing PVPh have been reported to be miscible over the wide range of blend composition in the amorphous state. It is also reported that PVPh is analogous to a good solvent to enhance miscibility of two immiscible polymers.²⁸ Inoue et al. have found a reversible thinning–thickening phenomenon for syndiotactic P(3HB)/PVPh and atactic P(3HB)/PVPh blends systems with specific composition in the aqueous solution.^{29,30} In this study, the specific interaction and thermal properties were characterized for P(3HB-co-3HH)/PVPh binary blends. The miscibility of the blends was investigated by differential scanning calorimetry (DSC) and the hydrogen-bonding interaction is characterized by Fourier transform infrared spectroscopy (FTIR). Finally, the mechanical

Correspondence to: Y. Inoue (inoue.y.af@m.titech.ac.jp).

properties of the blends were characterized by tensile testing.

EXPERIMENTAL

Materials and sample preparation

P(3HB-*co*-3HH) with 3HH molar fraction 20 mol % was fractionated from the as-produced P(3HB-*co*-18 mol % 3HH) sample using the solvent/nonsolvent fractionation method as reported previously.²² The weight-average molecular weight and polydispersity of the P(3HB-*co*-20 mol % 3HH) sample were determined to be 2.76×10^5 and 1.82, respectively, by GPC measurements. Atactic PVPh ($M_w = 1.08 \times 10^4$, $P_d = 2.25$, lot no. 16824361) was supplied by the courtesy of Maruzen Petrochemical Co. Ltd.

The P(3HB-*co*-3HH)/PVPh blends were prepared by solution casting using acetone as the common solvent. The solution was cast on the Teflon Petri dish, allowing the solvent to evaporate at room temperature for 1 day, then drying in vacuum at 40°C for 1 week before the DSC and FTIR measurements.

Differential scanning calorimetry

DSC measurements were carried out on a Seiko DSC-220 assembled with SSC-580 thermal controller. 8–10 mg sample was encapsulated in an aluminum pan. The DSC thermogram was recorded from –50 to 200°C at a heating rate of 10°C/min. The glass transition temperature (T_g) was taken as the summit of the peak of the differentiated DSC (DDSC) curves.

Fourier-transform infrared spectroscopy

The films of the polymer blends for FTIR measurements were prepared by dropping the polymer blend solution on the surface of silicon wafer. Silicon wafer is transparent to IR incident beam and was used as substrate. The thickness of the film was carefully controlled to be thin enough to obey the Beer-Lambert law. FTIR spectra were recorded on a Perkin-Elmer Spectrum 2000 spectrometer using a minimum of 64 coadded scans at a resolution of 4 cm^{-1} . Nitrogen was used to purge CO₂ and gaseous water in the detector and sample compartments prior to and during the scans.

Tensile test

Tensile properties were measured at room temperature using an EZ test machine (Shimadzu Corp., Tokyo, Japan). The gauge length and crosshead speed were 22.25 mm and 20 mm/min, respectively. The sample thickness was ~ 0.1 mm. At least five samples were tested and the average was used.

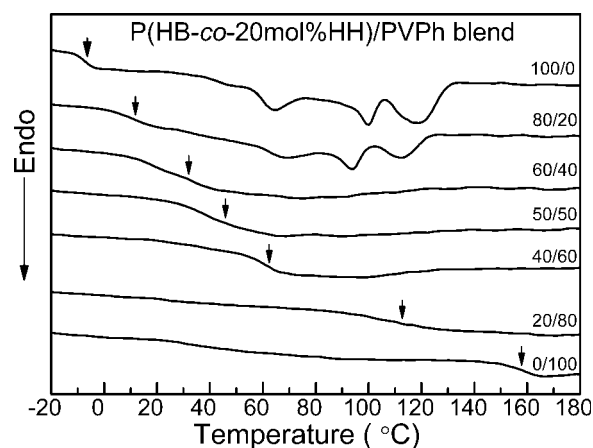


Figure 1 DSC thermograms of pure P(3HB-*co*-20 mol % 3HH), pure PVPh, and binary P(3HB-*co*-20 mol % 3HH)/PVPh blends of various compositions: first heating scan, heating rate = 10°C/min.

RESULTS AND DISCUSSION

DSC measurements

Differential scanning calorimetry (DSC) is extensively used to investigate the miscibility of the polymer blends. A composition-dependent single glass transition is an indication of fully miscible blend at a dimensional scale between 20 and 40 nm. Figure 1 shows the DSC thermograms of the pure P(3HB-*co*-20 mol % 3HH), pure PVPh, and P(3HB-*co*-20 mol % 3HH)/PVPh blends with various composition recorded during the first heating scan. As clearly shown in Figure 1, pure P(3HB-*co*-20 mol % 3HH) and pure PVPh exhibit a single glass transition at –7°C and 160.5°C, respectively. All the P(3HB-*co*-20 mol % 3HH)/PVPh blends showed a composition-dependent single glass transition and the T_g value increases with the increase of PVPh content in the blends.

The dependence of T_g on the composition of miscible P(3HB-*co*-3HH)/PVPh blend can be evaluated by the Wood's equation (eq. (1)),³¹

$$T_g = ((W_1 T_{g1} + kW_2 T_{g2}) / (W_1 + kW_2)) \quad (1)$$

where T_g is the glass transition temperature of the blends, T_{g1} and T_{g2} are those of pure components, P(3HB-*co*-3HH) and PVPh, respectively, and k is an adjustable fitting parameter that semiquantitatively describes the strength of intermolecular interaction. W is the weight fraction. The good agreement of observed T_g value with that calculated from the Wood's equation with k value of 0.45 as shown in Figure 2 indicates that P(3HB-*co*-3HH) and PVPh polymer form single homogeneous amorphous phase; i.e., the two polymers are fully miscible in the amorphous phase.

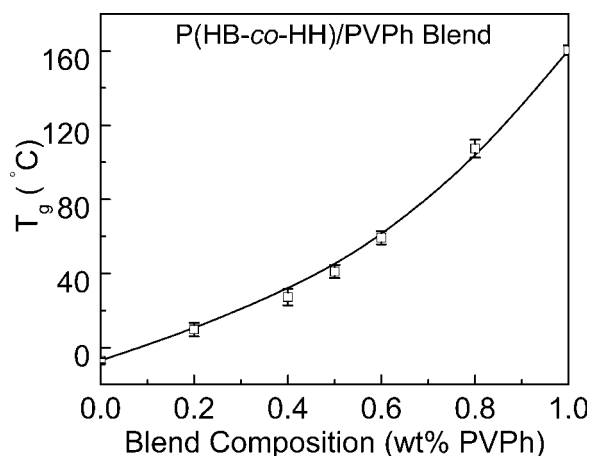


Figure 2 Relationship between the glass transition temperature (T_g) and the composition of P(3HB-co-3HH)/PVPPh blends. The solid line is the calculated T_g values based on the Wood's equation with k value of 0.45.

In Figure 1, the melting peak was observed only in the thermograms of pure P(3HB-co-20 mol % 3HH) and P(3HB-co-20 mol % 3HH)/PVPPh blend with weight composition of 80/20. The sample 80/20 exhibit multi-melting peaks similar to pure P(3HB-co-3HH), but each melting point and the melting enthalpy decreased when compared with pure P(3HB-co-3HH). The above results indicate that the specific intermolecular interaction between the two polymers leads the polymer chains diffusing into each other's phase, which causes the change of crystallization behavior.

FTIR measurements

Infrared spectroscopy has been proven to be a highly effective means of investigating specific interaction between various chemical groups of the polymers. In this study, two main bands, the carbonyl vibration region ($1650\text{--}1790\text{ cm}^{-1}$) and the hydroxyl stretching region ($2800\text{--}3800\text{ cm}^{-1}$), in FTIR spectra were investigated because the variation of band intensity, peak width, and position is clearly depending on the blend composition.

Figure 3 shows the infrared spectra of the carbonyl vibration region ranging from 1650 to 1790 cm^{-1} for the P(3HB-co-3HH), PVPh, and their blends measured at room temperature. The carbonyl vibration for the pure P(3HB-co-3HH) is split into two bands, absorptions of the carbonyl groups in the amorphous and crystalline phases, at 1724 and 1740 cm^{-1} , respectively. These bands can be decomposed into two Gaussian peaks, with areas corresponding to the amorphous carbonyl (1740 cm^{-1}) and crystalline carbonyl (1724 cm^{-1}) absorption. The accurate wavenumber of the amorphous band was determined from the spectrum of the fully amorphous sample

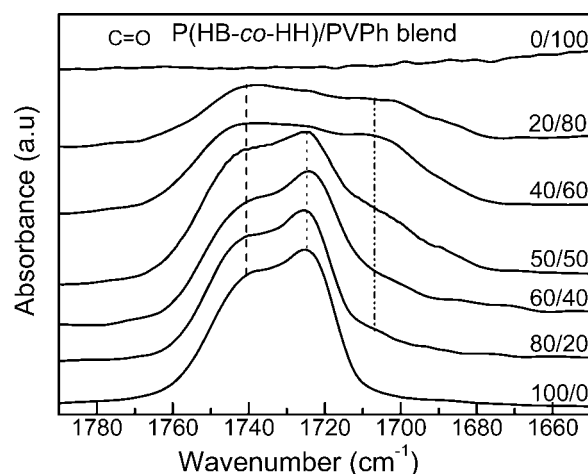


Figure 3 Infrared spectra in the carbonyl vibration band of P(3HB-co-3HH)/PVPPh blends with different compositions recorded at room temperature.

observed at 185°C . In the carbonyl-stretching region of the P(3HB-co-3HH)/PVPPh binary blends, a new absorption band appeared at the lower wavenumber side centered at 1709 cm^{-1} , which can be attributed to the hydrogen-bonded carbonyl vibration, because PVPh shows no absorption in this region. The relative intensity of the hydrogen-bonded carbonyl band increases with PVPh weight content in the blends, while those of the free carbonyl group band (consisting of amorphous and crystalline components) decreases. These results indicate the formation of hydrogen bonds between the hydroxyl groups of PVPh and the carbonyl groups of P(3HB-co-3HH).

Figure 4 shows the infrared spectra of hydroxyl stretching region of the pure P(3HB-co-3HH), PVPh, and various P(3HB-co-3HH)/PVPPh blends ranging from 2800 to 3800 cm^{-1} measured at room temperature. As shown in Figure 4, pure PVPh exhibits two

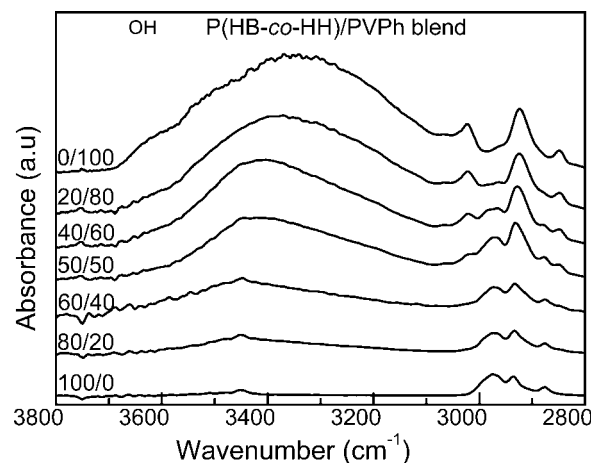


Figure 4 Infrared spectra in the hydroxyl stretching band of P(3HB-co-3HH)/PVPPh blends with different compositions recorded at room temperature.

bands in the hydroxyl stretching region of the infrared spectrum. The free hydroxyl group absorption is located at 3525 cm^{-1} , while the hydrogen bonded hydroxyl group absorption showed a broad band centered at 3350 cm^{-1} because of wide distribution of hydrogen-bonded hydroxyl group. Free hydroxyl group, which for P(3HB-co-3HH), only a very weak band centered at 3446 cm^{-1} is observed in this region, which originated from the vibration of the hydroxyl group in the chain terminal of P(3HB-co-3HH). Because of its low intensity compared to that of the band of PVPh in this region, the contribution of this band to the spectra of the blends is reasonably negligible when the PVPh weight content is not too low. For the P(3HB-co-3HH)/PVPh blends, a shoulder appeared at 3390 cm^{-1} in the hydroxyl stretching region of the infrared spectrum, and the relative intensity of this shoulder band increases with the increase of PVPh weight content. This result reflects that new distribution of the hydroxyl-hydroxyl and the hydroxyl-carbonyl specific interactions exists in the blend system. The average strength of the intermolecular hydrogen bonding interaction can be obtained from frequency difference ($\Delta\nu$) between the hydrogen-bonded hydroxyl absorption and the free hydroxyl absorption. From the blend containing 80 wt % of PVPh, the intermolecular hydrogen-bonded band at 3390 cm^{-1} ($\Delta\nu = 135\text{ cm}^{-1}$) shifted to 3350 cm^{-1} ($\Delta\nu = 175\text{ cm}^{-1}$), indicating that the strength of the hydroxyl-hydroxyl specific interaction of PVPh is stronger than that of the intermolecular hydrogen bonding interaction between the carbonyl group of P(3HB-co-3HH) and the hydroxyl group of PVPh. Quantitative analysis of the hydroxyl stretching region of polymer blends is too difficult, because of (1) very broad stretching region, (2) the extensive overlap of the bands of interest, and (3) the molar absorptivities of the components being a strong function of wavenumber and temperature.

Curve-fitting analysis of the fraction of hydrogen-bonded carbonyl group

The existence of intermolecular hydrogen-bonding interaction between the carbonyl group of P(3HB-co-3HH) and the hydroxyl group of PVPh were confirmed in the FTIR spectrum of their blend system. On the basis of the Beer-Lambert law, by using curve-fitting program, the carbonyl vibration region of the pure P(3HB-co-3HH) and P(3HB-co-3HH)/PVPh blends system can be quantitatively analyzed to three components centered at 1709 , 1724 , and 1740 cm^{-1} , corresponding to the hydrogen-bonded, the crystalline, and the amorphous states, respectively. A lot of reports have been discussed in similar blends system for a quantitative evaluation of

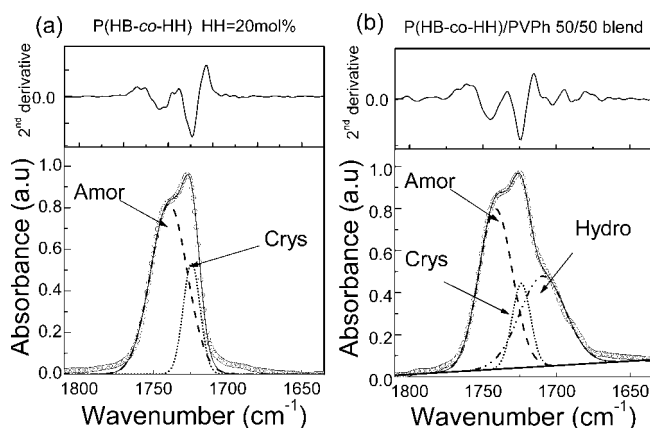


Figure 5 Experimental and curve-fitting results of infrared spectra in the carbonyl stretching region for pure P(3HB-co-20 mol % 3HH) (a) and binary P(3HB-co-20 mol % 3HH)/PVPh 50/50 blend (b). Dash line Amor.: amorphous component; shot dot line Crys.: crystalline component; dash dot line Hydr.: hydrogen-bonded component; solid line: curve-fitted result; symbol (O): experimental spectrum.

the fraction of intermolecular hydrogen-bonding interaction.^{25,32,33}

As an example, the results of curve-fitting for the pure P(3HB-co-3HH) and P(3HB-co-3HH)/PVPh 50/50 wt %/wt % blend were shown in Figure 5. The excellent agreement between the experimental spectra, second derivative of the curve, and fitted spectra indicates the reliability of this curve-fitting technique. In the blend system, the carbonyl absorption band was divided into three parts, the amorphous, the crystalline, and the hydrogen-bonded, with Gaussian line-shape obtained for all the cases. During fitting progress, the peak position of amorphous components, crystalline components, and hydrogen bonded bands were fixed, putting the peak shape, widths, and heights of the three bands as the adjustable parameters.

The fraction of the hydrogen-bonded carbonyl group can be calculated by the following equation

$$F_b = A_b / (A_b + \gamma_{b/a}A_a + \gamma_{b/c}A_c) \quad (2)$$

where A_a , A_c , and A_b denote the integrated peak areas corresponding to the amorphous (a), crystalline (c), and hydrogen-bonded carbonyl bands (b), respectively. the factors $\gamma_{b/a}$ and $\gamma_{b/c}$ are absorption ratios that taken into account the differences between the absorptivities of the hydrogen-bonded (b) and amorphous (a) carbonyl group and between those of the hydrogen-bonded (b) and crystalline (c) carbonyl group, respectively. The ratios $\gamma_{b/a}$ and $\gamma_{b/c}$ also can be calculated on the basis of Beer-Lambert law, by measuring the film thickness of the FTIR

TABLE I
Curve-Fitting Results of Binary P(3HB-co-3HH)/PVPh Blends at Room Temperature

P(HB-co-HH)/ PVPh (wt %)	Free C=O									Fraction of hydrogen- bonded (%)
	Amorphous			Crystalline			Hydrogen-bonded C=O			
	ν (cm^{-1})	$w_{1/2}$ (cm^{-1})	Area frac (%)	ν (cm^{-1})	$w_{1/2}$ (cm^{-1})	Area frac (%)	ν (cm^{-1})	$w_{1/2}$ (cm^{-1})	Area frac (%)	
100/0	1739	28.54	78.39	1724	12.75	21.61	–	–	–	–
80/20	1739	26.04	62.57	1724	12.25	19.45	1710	32.50	17.98	12.73
60/40	1739	26.70	59.35	1724	14.37	15.52	1710	37.15	25.13	19.98
50/50	1739	26.77	57.75	1724	14.69	5.10	1710	36.45	37.15	28.27
40/60	1739	30.24	51.32	1724	12.69	3.29	1710	32.31	45.39	35.65
20/80	1739	30.12	51.27	1724	8.64	1.33	1710	35.17	47.40	37.53

sample. In this study, we used the value $\gamma_{b/a} = \gamma_{b/c} = 1.5$, which has been proposed as an appropriate absorptivity ratio for similar polyester systems.^{25,32,33}

The results of the curve-fitting of P(3HB-co-3HH)/PVPh blends are summarized in Table I. The fraction of the hydrogen-bonded carbonyl group increases with PVPh content in the blend system. But the fraction of both the amorphous and crystalline phase decreases with increase of PVPh content, indicating that the formation of the hydrogen-bond between the hydroxyl group of PVPh and the carbonyl group of P(3HB-co-3HH) strongly suppresses the crystallization of P(3HB-co-3HH) chains. These results agree well with the DSC results. Although clear melting behavior was not observed for the blends with PVPh content above 40% in DSC measurements, the FTIR spectra revealed the presence of a trace crystalline phase. This discrepancy may be partly due to that the DSC melting peak reflects dominantly the long-range order, while the FTIR crystalline band reflects relatively short-range order as well as long-range-order. As shown in Figure 2, the T_g value of P(3HB-co-3HH)/PVPh blends increases with the increase of PVPh content. Because of the formation of strong

intermolecular hydrogen bonding interaction, as confirmed here by FTIR spectra, the resulted two associated polymer chains, that is, P(3HB-co-3HH)/PVPh pairs diffuse into each other's phase and become homogeneous in the amorphous phase.

Mechanical properties

The results of tensile testing for pure P(3HB-co-3HH), P(3HB-co-3HH)/PVPh 90/10 wt %/wt %, and P(3HB-co-3HH)/PVPh 80/20 wt %/wt % blends are shown in Figure 6. The tensile strength of the blends decreases with the increase of PVPh weight contents, which is caused by the decrease of P(3HB-co-3HH) crystallinity in blending with PVPh. As mentioned in the above discussion, the crystallinity is strongly influenced because of the formation of hydrogen bonding interaction. Simultaneously, compared with pure P(3HB-co-3HH), the strain also decreases with the increase of PVPh weight content. The segmental mobility of P(3HB-co-3HH) reduced, probably because of the formation of intermolecular hydrogen bonding interaction with less mobile PVPh segments in the amorphous phase. In DSC results, the 80/20 wt %/wt % blend showed a glass transition at the temperature very near to the room temperature, the amorphous phase is almost in the glassy state at room temperature, thus, the yield stress showed a little increase even compared to pure P(3HB-co-3HH). For the blends with PVPh content higher than 20 wt %, it was failed to measure the mechanical properties, due to the intrinsic brittleness of the blends.

CONCLUSIONS

The thermal properties and the formation of strong intermolecular hydrogen bonding interaction between P(3HB-co-3HH) and PVPh in their binary blends were investigated by DSC and FTIR. In the DSC measurements, a compositional dependent single glass transition was observed, indicating that the P(3HB-co-3HH)/PVPh binary blend system is fully

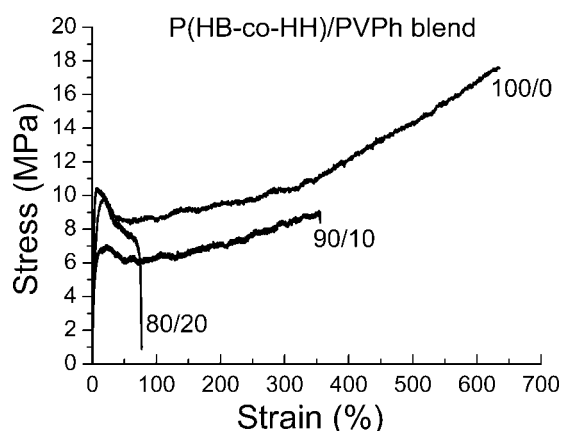


Figure 6 Stress-strain curves of pure P(3HB-co-20 mol % 3HH) and the P(3HB-co-20 mol % 3HH)/PVPh binary blends with 90/10 and 80/20 compositions.

miscible in the amorphous phase. The formation of strong intermolecular hydrogen bonding interaction was demonstrated by FTIR measurements. In tensile testing, both the tensile stress and strain decrease with the increase of PVPh weight content in the blends. In conclusion, the thermal and mechanical properties of the P(3HB-co-3HH) were greatly modified by blending with PVPh via formation of the strong hydrogen bonds.

References

1. Utracki, L. A. *Polymer Alloy and Blends*; Hanser: New York, 1989.
2. Olabisi, O.; Robenson, L. M.; Shaw, M. T. *Polymer-Polymer Miscibility*; Academic Press: New York, 1979.
3. Hill, D. J. T.; Whittaker, A. K.; Wong, K. W. *Macromolecules* 1999, 32, 5285.
4. Inoue, Y.; Yoshio, N. *Prog Polym Sci* 1992, 17, 571.
5. Hexig, B.; He, Y.; Asakawa, N.; Inoue, Y. *J Polym Sci Part B: Polym Phys* 2004, 42, 2971.
6. Byrom, D. *Trends Biotechnol* 1987, 5, 246.
7. Tsuge, T.; Saito, Y.; Kikkawa, Y.; Hiraishi, T.; Doi, Y. *Macromol Biosci* 2004, 4, 238.
8. Shimamura, E.; Scandola, M.; Doi, Y. *Macromolecules* 1994, 27, 4429.
9. Kunioka, M.; Kawaguchi, Y.; Doi, Y. *Appl Microbiol Biotechnol* 1989, 30, 569.
10. Avella, M.; Martuscelli, E. *Polymer* 1988, 29, 1731.
11. Avella, M.; Martuscelli, E.; Greco, P. *Polymer* 1991, 32, 1647.
12. Marand, H.; Collins, M. *ACS Polym Prepr* 1990, 31, 552.
13. Edie, S. L.; Marand, H. *ACS Polym Prepr* 1991, 32, 329.
14. McCarthy, S. P.; Gross, R.; *Proceedings of Environmentally Degradable Polymers: Technical, Business, and Public Perspectives*; Chelmsford, MA, 1991.
15. Dave, B.; Parikh, M.; Reeves, M. S.; Gross, R. A.; McCarthy, S. P. *Polym Mater Sci Eng* 1990, 63, 726.
16. Dubini, P. E.; Beltrame, P. L.; Canetti, M.; Seves, A.; Marcardalli, B.; Martuscelli, E. *Polymer* 1993, 34, 996.
17. Sadocco, P.; Canetti, M.; Seves, A.; Martuscelli, E. *Polymer* 1993, 34, 3368.
18. Iriondo, P.; Iruin, J. J.; Frenandez-Berridi, M. J. *Macromolecules* 1996, 29, 5605.
19. Greco, P.; Martuscelli, E. *Polymer* 1989, 30, 1475.
20. Chiu, H. J.; Chen, H. L.; Lin, T. L.; Lin, J. S. *Macromolecules* 1999, 32, 4969.
21. Park, S. J.; Ahn, W. S.; Green, P. R.; Lee, S. Y. *Biomacromolecules* 2001, 2, 248.
22. Watanabe, T.; He, Y.; Fukuchi, T.; Inoue, Y. *Macromol Biosci* 2001, 1, 75.
23. Coleman, M. M.; Lichkus, A. M.; Painter, P. *Macromolecules* 1989, 22, 586.
24. Wang, J.; Cheng, K. M.; Mi, Y. *Polymer* 2002, 43, 1357.
25. Li, D.; Brisson, J. *Polymer* 1998, 39, 793.
26. Coleman, M. M.; Painter, P. C. *Prog Polym Sci* 1995, 20, 1.
27. Li, L.; Chan, C. M.; Wang, L. T.; Xiang, M. L.; Jiang, M. *Macromolecules* 1998, 31, 7248.
28. Kuo, S. W.; Chan, S. C.; Chang, F. C. *Polymer* 2002, 43, 3653.
29. He, Y.; Li, J.; Shuai, X.; Inoue, Y. *Macromolecules* 2001, 34, 8166.
30. Li, J.; He, Y.; Inoue, Y. *Polymer J* 2002, 34, 562.
31. Wood, L. A. *J Polym Sci* 1958, 28, 319.
32. Li, D.; Brisson, J. *Polymer* 1998, 39, 801.
33. Coleman, M. M.; Graf, J. F.; Painter, P. C. *Specific Interactions and the Miscibility of Polymer Blends*; Technomic: Lancaster, PA, 1991.